inorganics

MDPI

Article

Thermodynamic Properties and Reversible Hydrogenation of $LiBH_4$–Mg_2FeH_6 Composite Materials

Guanqiao Li [1,*], Motoaki Matsuo [2], Shigeyuki Takagi [1], Anna-Lisa Chaudhary [3], Toyoto Sato [1], Martin Dornheim [3] and Shin-ichi Orimo [1,4]

1 Institute for Materials Research, Tohoku University, Sendai 980-8577, Japan; shigeyuki.takagi@imr.tohoku.ac.jp (S.T.); toyoto@imr.tohoku.ac.jp (T.S.); orimo@imr.tohoku.ac.jp (S.O.)
2 Department of Nanotechnology for Sustainable Energy, School of Science and Technology, Kwansei Gakuin University, Sanda 669-1337, Japan; matsuo35@kwansei.ac.jp
3 Department of Nanotechnology, Institute of Materials Research, Helmholtz-Zentrum Geesthacht, D-21502 Geesthacht, Germany; anna-lisa.chaudhary@hzg.de (A.-L.C.); martin.dornheim@hzg.de (M.D.)
4 WPI-Advanced Institute for Materials Research (WPI-AIMR), Tohoku University, Sendai 980-8577, Japan
* Correspondence: likk@imr.tohoku.ac.jp

Received: 8 October 2017; Accepted: 2 November 2017; Published: 16 November 2017

Abstract: In previous studies, complex hydrides $LiBH_4$ and Mg_2FeH_6 have been reported to undergo simultaneous dehydrogenation when ball-milled as composite materials $(1 - x)LiBH_4 + xMg_2FeH_6$. The simultaneous hydrogen release led to a decrease of the dehydrogenation temperature by as much as 150 K when compared to that of $LiBH_4$. It also led to the modified dehydrogenation properties of Mg_2FeH_6. The simultaneous dehydrogenation behavior between stoichiometric ratios of $LiBH_4$ and Mg_2FeH_6 is not yet understood. Therefore, in the present work, we used the molar ratio x = 0.25, 0.5, and 0.75, and studied the isothermal dehydrogenation processes via pressure–composition–isothermal (PCT) measurements. The results indicated that the same stoichiometric reaction occurred in all of these composite materials, and x = 0.5 was the molar ratio between $LiBH_4$ and Mg_2FeH_6 in the reaction. Due to the optimal composition ratio, the composite material exhibited enhanced rehydrogenation and reversibility properties: the temperature and pressure of 673 K and 20 MPa of H_2, respectively, for the full rehydrogenation of x = 0.5 composite, were much lower than those required for the partial rehydrogenation of $LiBH_4$. Moreover, the x = 0.5 composite could be reversibly hydrogenated for more than four cycles without degradation of its H_2 capacity.

Keywords: complex hydride; composite material; hydrogen storage

1. Introduction

Boron-based complex hydrides MBH_4 (M = Li, Na, and K), which consist of an M^+ cation and a $[BH_4]^-$ complex anion, have high gravimetric H_2 densities (7.7–18.4 mass %); therefore, these materials have the potential to be used as hydrogen storage materials [1–3]. However, MBH_4 are thermodynamically stable and the hydrogenation is difficult to achieve under mild temperatures and pressures. For example, when undergoing the following Reaction (1), the dehydrogenation temperature of $LiBH_4$ at 0.1 MPa H_2 has been estimated to be 683 K on the basis of enthalpy ΔH and entropy ΔS changes of 66.6 kJ/(mole of H_2) and 97.4 J/K(mole of H_2), respectively [4]. In practice, significant dehydrogenation only occurs at temperatures greater than 700 K. In addition, partial rehydrogenation of $LiBH_4$ requires a much higher pressure and temperature of 35 MPa and 873 K.

$$LiBH_4 \rightleftharpoons LiH + B + (3/2)H_2 \quad (1)$$

Combining borohydrides with metallic hydrides (e.g., MgH_2) or complex hydrides (e.g., Mg_2NiH_4) has been proven to be effective at modifying the dehydrogenation properties of MBH_4. The reactions between MBH_4 and the partner hydrides in these composite materials can produce the stable boride MgB_2 or $MgNi_{2.5}B_2$ that results in a decrease of the dehydrogenation temperature of $LiBH_4$ [5–11]. Therefore, in a previous study, we have tried to bring down the dehydrogenation temperature of $LiBH_4$ by combining it with a transition-metal-based complex hydride, Mg_2FeH_6. We ball-milled the two complex hydrides over a large composition range: $(1 - x)LiBH_4 + xMg_2FeH_6$ ($0.25 \leq x \leq 0.9$) [12–15]. The dehydrogenation properties were investigated using a dynamic measurement: thermogravimetry–mass spectrometry (TG–MS). It was observed that although the thermodynamic stabilities of $LiBH_4$ and Mg_2FeH_6 differed substantially, they underwent dehydrogenation simultaneously when heated up during the TG–MS analysis, by which the dehydrogenation temperature of the composite materials was lowered by, at most, 150 K when compared to that of $LiBH_4$. In addition to the dehydrogenation properties of $LiBH_4$, those of Mg_2FeH_6 were also modified; Mg_2FeH_6 no longer underwent independent dehydrogenation, and the temperature of the simultaneous dehydrogenation shifted closer to that of pure Mg_2FeH_6, both continuously and with an increasing ratio x.

The dehydrogenation process of $(1 - x)LiBH_4 + xMg_2FeH_6$ is special when compared to the processes of other composite materials, e.g., $2LiBH_4 + MgH_2$ [16]. The dehydrogenation behavior of MgH_2 was unaffected by its combination with $LiBH_4$; furthermore, a stoichiometric reaction between $LiBH_4$ and MgH_2 existed, the dehydrogenation temperature of which would not be affected by the composition ratio in the composite materials. However, in the case of $(1 - x)LiBH_4 + xMg_2FeH_6$, the properties of both $LiBH_4$ and Mg_2FeH_6 were modified and the stoichiometric reaction between these two complex hydrides at a specific composition ratio was not yet understood. We considered that the stoichiometric reaction was hidden in the continuous hydrogen releasing events in the dynamic TG–MS measurements, where the thermodynamic and kinetic factors both affected the dehydrogenation process.

Besides our study, the research on $LiBH_4 + Mg_2FeH_6$ composite materials has been conducted on $LiBH_4$-rich compositions only. The reaction processes investigated by various dynamic measurement methods (for example, differential scanning calorimetry (DSC)) has been explained as Mg_2FeH_6 dehydrogenating to form elemental Mg and Fe, followed by the Mg and Fe reacting with $LiBH_4$ and thereby destabilizing it thermodynamically. Because of the absence of studies on any Mg_2FeH_6-rich compositions, the simultaneous dehydrogenation was not discovered [17,18]. In addition, Ghaani et al. used an isothermal method (i.e., the pressure–composition–isothermal (PCT) measurement) to study the dehydrogenation process of $2LiBH_4 + Mg_2FeH_6$. Here, it was found that $LiBH_4$ and Mg_2FeH_6 react with each other; however, unreacted $LiBH_4$ was apparent using this composition ratio [19]. Whether the reaction between $LiBH_4$ and Mg_2FeH_6 changes with variations in composition ratio is unclear, and whether an optimal composition ratio exists at which a stoichiometric reaction occurs without independent dehydrogenation of the parent complex hydrides remains unknown.

In this study, to confirm the stoichiometric reaction between Mg_2FeH_6 and $LiBH_4$, and the optimal composition ratios for it, we used PCT measurements to evaluate the isothermal dehydrogenation processes of $(1 - x)LiBH_4 + xMg_2FeH_6$. Among a large range of composition ratios, the focus was on three in the present study: x = 0.25, 0.5, and 0.75. TG–MS measurements done in our previous study revealed that x = 0.5 was a critical composition. Composites with $x \geq 0.5$ exhibited a single dehydrogenation event, whereas composites with $x < 0.5$ underwent multiple events involving both simultaneous dehydrogenation of $LiBH_4$ and Mg_2FeH_6, and individual dehydrogenation of $LiBH_4$. We considered that the optimal ratio for the stoichiometric reaction could be deduced from these representative compositions. After deciding on the optimal ratio, its effect on the modification of the reversible hydrogenation properties of the composite materials were investigated.

2. Results

2.1. Optimal Composition Ratio for the Stoichiometric Reaction between $LiBH_4$ and Mg_2FeH_6

The PCT results obtained at 643 K for the composites (x = 0.25, 0.5, and 0.75; temperatures were slightly different within each measurement) are shown in Figure 1. Although only one dehydrogenation event was observed for the x = 0.5 and 0.75 composites in the dynamic TG–MS measurements, the PCT results revealed two and three thermodynamically independent reactions, respectively. For x = 0.25, three independent reactions were observed, similar to the TG–MS results in which multiple dehydrogenation events appeared. The first and second dehydrogenation reactions of all of these compositions exhibited the same equilibrium pressure of 1.85 MPa and 0.85 MPa, which indicates that these compositions have undergone similar reaction pathways.

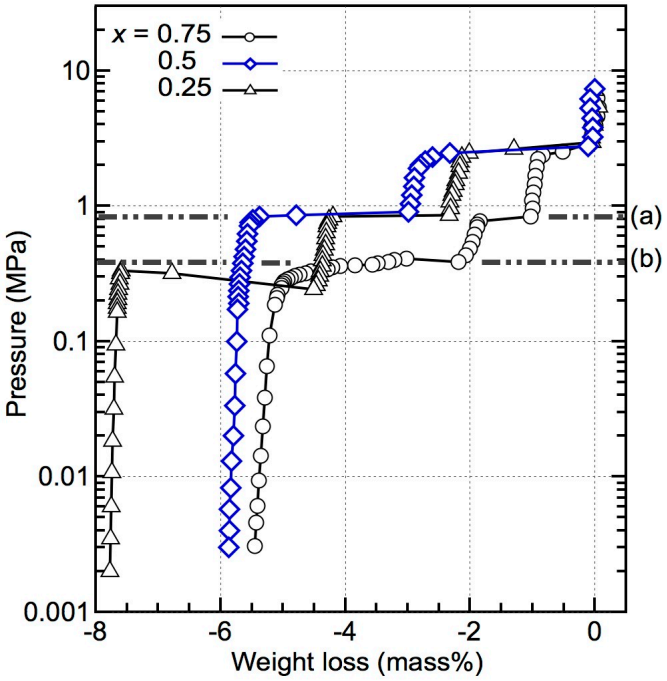

Figure 1. Pressure–composition–isothermal (PCT) results for $(1 - x)LiBH_4 + xMg_2FeH_6$ (x = 0.25, 0.5, and 0.75) at 643 K. The temperatures are slightly different within each measurement. The first and second reactions in all the compositions exhibit the same equilibrium pressures of 1.85 MPa and 0.85 MPa, respectively. Line (a) represents the equilibrium pressure of the dehydrogenation of MgH_2, according to Refs. [20,21]; line (b) represents the equilibrium pressure of the dehydrogenation of Mg_2FeH_6, according to Refs. [22–24].

To determine the reaction pathway, the materials were quenched under H_2 pressure after each thermodynamically independent reaction and each phase was identified using X-ray diffraction (XRD). The XRD results for the x = 0.5 composite after each reaction are shown in Figure 2. After the first reaction at 1.85 MPa H_2, the diffraction peaks of Mg_2FeH_6 were no longer apparent, whilst the intensity of the diffraction peak of Fe increased. Furthermore, peaks attributable to MgH_2 appeared, accompanied by several small broad peaks of an unclear phase. The results indicate that Mg_2FeH_6 was fully dehydrogenated. After the second reaction at 0.85 MPa H_2, the diffraction peaks of MgH_2 transitioned to those of Mg. The small broad unclear peaks were not prominent but were still present, indicating that this phase did not participate in the second reaction. The presence of $LiBH_4$ was not confirmed by XRD due to its weak diffraction intensity compared to the other reactants as well as the amorphisation after ball-milling. Because direct dehydrogenation of Mg_2FeH_6 cannot produce MgH_2;

we considered that $LiBH_4$ reacted with Mg_2FeH_6 in the first reaction. Also, we used scanning electron microscopy (SEM) to characterize the presence of $LiBH_4$ before and after the first reaction.

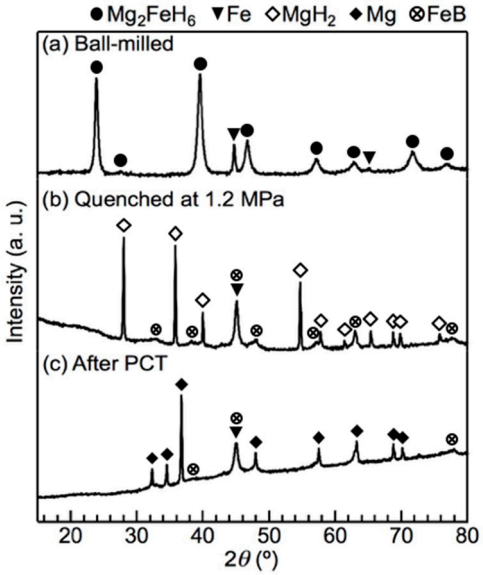

Figure 2. X-ray diffraction (XRD) profiles of the x = 0.5 composite during the pressure–composition–isothermal (PCT) measurement at 643 K: (**a**) the ball-milled material before the PCT measurement; (**b**) the material quenched at 1.2 MPa, which is the pressure between the first isothermal reaction at 1.85 MPa and the second one at 0.85 MPa; and (**c**) the material after the PCT measurement. As a result of Fe in the material, the baseline tilted at high angles. The strongest diffraction peak of LiH overlapped with that of Fe at 44°.

The backscattering images (BSE) and energy-dispersive X-ray spectroscopy (EDX) analysis results obtained before the PCT measurements and after the first reaction are shown in Figure 3. Before the PCT measurement, the composite material was a uniform mixture; separate $LiBH_4$ and Mg_2FeH_6 particles were not observed at about 100-nm scale. After the first isothermal reaction at 1.85 MPa, the composite became an obvious mixture. A large blank area was observed where no B, Fe, or Mg were detected, suggesting that this area was possibly composed of the dehydrogenation product of $LiBH_4$: LiH. These results complement the XRD results, indicating that both $LiBH_4$ and Mg_2FeH_6 underwent dehydrogenation in the first reaction. Element mapping of Fe and B showed significant overlap, and the particle size was of the order of several nanometers, indicating the possible formation of iron boride. A 1:1 reaction ratio between $LiBH_4$ and Mg_2FeH_6 in the first isothermal reaction suggests that FeB is a possible iron boride product. The recognized diffraction patterns in the XRD results can be attributed to FeB (orthorhombic, *Cmcm*), but the very broad peaks made the phase identification difficult. Because of the overlapping of the strongest diffraction peaks of Fe (cubic, *Im-3m*) and FeB, it is hard to rule out the existence of Fe. Therefore, we still keep it in the reaction of Equation (2). The formation of FeB is crucial for the reaction between $LiBH_4$ and Mg_2FeH_6. The estimated enthalpy change ΔH and entropy change ΔS for the reaction ($LiBH_4 + Mg_2FeH_6 \rightarrow LiH + 2MgH_2 + FeB + 5/2H_2$) is 64 kJ/(mol of H_2) and 125 J/K(mole of H_2) , respectively. According to the theoretical value, the equilibrium pressure at 643 K would be 2.1 MPa [23,25–27]. It is very close to the experimental data 1.85 MPa.

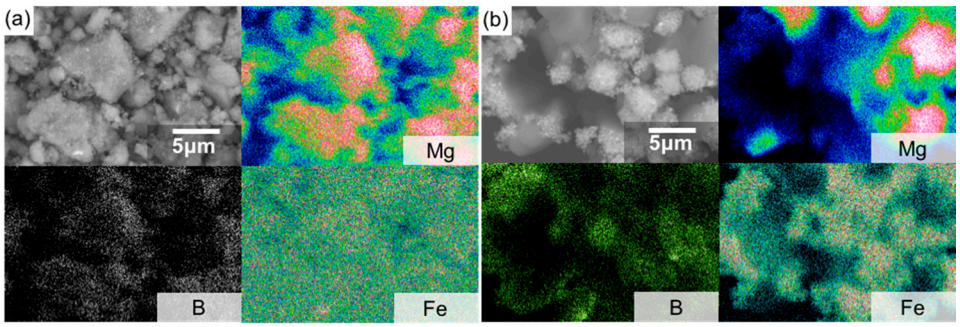

Figure 3. Backscattered electron (BSE) images and energy-dispersive X-ray spectroscopy (EDX) analyses of the $x = 0.5$ composite: (**a**) the material after ball milling was a uniform mixture of $LiBH_4$ and Mg_2FeH_6; (**b**) the material quenched at 1.2 MPa during the PCT measurement exhibited black areas, possibly LiH. These analyses indicate that $LiBH_4$ dehydrogenated simultaneously with Mg_2FeH_6 during the first isothermal reaction at 1.85 MPa.

On the basis of the phase identification results and the equilibrium pressure of the dehydrogenation reaction of MgH_2 calculated from previously reported thermodynamic data [20,21], Mg_2FeH_6 and $LiBH_4$ clearly reacted during the first reaction (Equation (2)), whereas the second reaction (Equation (3)) was the dehydrogenation of MgH_2.

$$LiBH_4 + Mg_2FeH_6 \rightarrow LiH + 2MgH_2 + (Fe, FeB) + 5/2H_2 \quad (2)$$

$$MgH_2 \rightarrow Mg + H_2 \quad (3)$$

The theoretical weight loss due to hydrogen release of Reactions (2) and (3) is 3.8 mass % and 3.0 mass %, respectively. This correlates well with the dehydrogenation of MgH_2 in the second reaction very well. However, the actual weight loss of the first reaction was only 3 mass %, and this deviation could be due to the residual Fe present from Mg_2FeH_6 synthesis.

As shown in Figure 4a, for $x = 0.25$, the phases changes at the first and second reaction were almost the same as those of $x = 0.5$, except for the presented diffraction peaks of $LiBH_4$ after the second reaction. The theoretical weight loss of Reactions (2) and (3) in $x = 0.25$ would be 2.9 mass % and 2.3 mass %, respectively. The actual weight loss of 2.5 mass % and 2.0 mass % at the first and second reaction, respectively, correlate with the theoretical value. The results indicate that the same stoichiometric reaction between $LiBH_4$ and Mg_2FeH_6 occurred in $x = 0.25$, and the amount of $LiBH_4$ in this composition is excessive for the stoichiometric reaction. An additional reaction with an incubation process occurred after the dehydrogenation of MgH_2, and diffraction peaks of MgB_2 appeared after this reaction. Therefore, the final isothermal reaction appears to be between $LiBH_4$ and Mg, as shown in Equation (4).

$$2LiBH_4 + Mg \rightarrow 2LiH + MgB_2 + 3H_2 \quad (4)$$

In the case of $x = 0.75$, after the dehydrogenation of MgH_2, diffraction peaks of Mg_2FeH_6 were still observed and finally disappeared after the last reaction, as shown in Figure 4b. Therefore, the last reaction can be attributed to the dehydrogenation of any residual Mg_2FeH_6:

$$Mg_2FeH_6 \rightarrow 2Mg + Fe + 3H_2 \quad (5)$$

The equilibrium pressure of the dehydrogenation of Mg_2FeH_6, calculated using reference data, also supports this interpretation [22,23]. The same stoichiometric reaction between $LiBH_4$ and Mg_2FeH_6, and the dehydrogenation of MgH_2, also occurred in $x = 0.75$. They contributed 1.4 mass % and 1.1 mass % weight loss in theoretical, and 1.1 mass % and 1.1 mass % in practice, respectively.

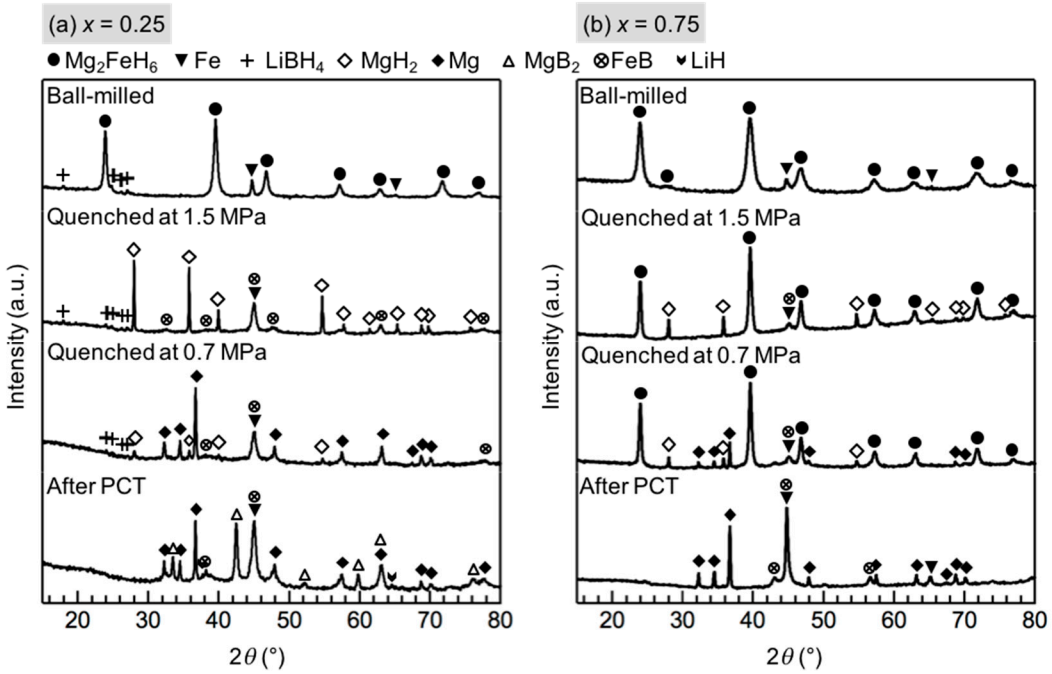

Figure 4. XRD profiles of (**a**) x = 0.25 and (**b**) x = 0.75 composite during the PCT measurement at 643 K: the ball-milled material before the PCT measurement; the material quenched at 1.5 MPa, which is the pressure after the first isothermal reaction at 1.85 MPa; the material quenched at 0.7 MPa, which is the pressure after the second isothermal reaction at 0.85 MPa; and after the PCT measurement. The strongest diffraction peak of LiH overlapped with that of Fe at 44°.

2.2. Reversible Hydrogenation Due to the Optimal Composition Ratio

After attempting rehydrogenation at different temperatures and pressures, we confirmed that full rehydrogenation was achievable at 673 K and 20 MPa H_2. The XRD profiles of the x = 0.5 composites before and after the rehydrogenation reaction at 673 K and 20 MPa H_2 are shown in Figure 5. Before rehydrogenation, the material released H_2 via a PCT program such that only Mg, LiH, Fe, and a small amount of FeB remained. After rehydrogenation, the XRD pattern showed the diffraction peaks of well-defined crystalline Mg_2FeH_6, indicating that Mg_2FeH_6 had been fully rehydrogenated. The weak diffraction peaks of α-Fe are attributed to the Fe located in the cores of the Mg_2FeH_6 grains, which, as reported previously [22,28], cannot be avoided. The diffraction peaks of Mg_2FeH_6 were sharp due to the fact that the heat treatment reduced the effect of the ball milling. $LiBH_4$ was not observed from XRD after ball-milling nor was its presence detected after rehydrogenation. Therefore, we used infrared (IR) spectroscopy to detect the presence of $LiBH_4$. As shown in Figure 6, the asymmetric stretching vibration mode and the bending mode of BH_4 appeared in the spectra of the rehydrogenated materials at approximately 2329 cm^{-1} and 1234–1095 cm^{-1}, respectively. The IR pattern correlated well with the data reported for pure $LiBH_4$ [29], demonstrating that $LiBH_4$ was present in the rehydrogenated material. The asymmetric stretching vibration of $[FeH_6]^{4-}$ at 1785 cm^{-1} was also seen [30].

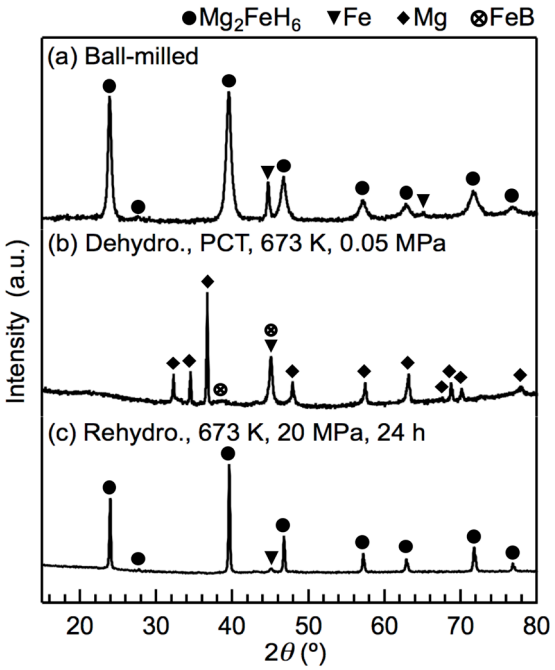

Figure 5. XRD profiles of the x = 0.5 composite before and after rehydrogenation at 673 K and 20 MPa H_2: (**a**) the material immediately after ball milling; (**b**) the material dehydrogenated at 673 K via a PCT measurement, and (**c**) the material rehydrogenated at 673 K and 20 MPa H_2.

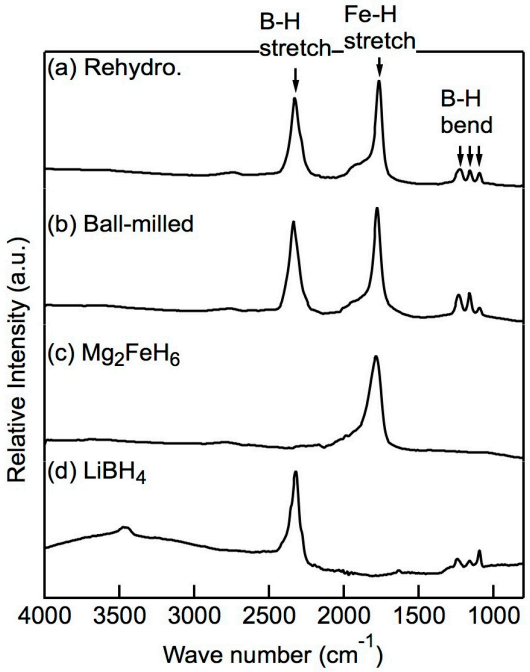

Figure 6. Infrared (IR) spectra of the x = 0.5 composite: (**a**) directly after ball-milling, (**b**) after rehydrogenation. The IR spectra of (**c**) pure Mg_2FeH_6 and (**d**) pure $LiBH_4$ are shown as references. The B–H vibration stretching at 2329 cm^{-1} and the bending vibration at 1234–1095 cm^{-1} demonstrate that $LiBH_4$ in the composite materials was successfully rehydrogenated.

The PCT plots of the dehydrogenation part during the reversible hydrogenation tests at 673 K are shown in Figure 7. The equilibrium pressure of the reaction between $LiBH_4$ and Mg_2FeH_6 at 6.8 MPa and that of the dehydrogenation reaction of MgH_2 at 1.8 MPa remained stable, indicating that the

properties of the composite materials did not degrade after cycling. The weight loss during each cycle did not decrease, suggesting that the composite material was fully rehydrogenated.

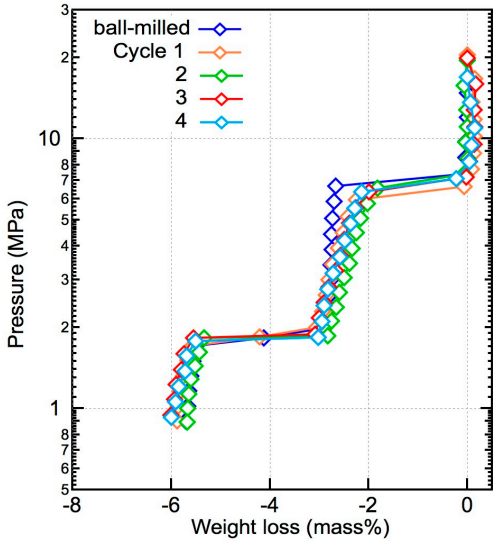

Figure 7. De/rehydrogenation reversibility of the $x = 0.5$ composite. The PCT plots were constructed for the dehydrogenation process after rehydrogenation in each cycle. After four cycles, the H_2 capacity of the materials remained the same.

3. Discussion

According to the PCT results, $(1 - x)LiBH_4 + xMg_2FeH_6$ (x = 0.25, 0.5, and 0.75) shared the same reaction between $LiBH_4$ and Mg_2FeH_6. This reaction was stoichiometric and its thermodynamic properties did not alter when excessive Mg_2FeH_6 or $LiBH_4$ were present. The optimal composition for this stoichiometric reaction was $x = 0.5$, which can be explained by the formation of FeB. The kinetics of FeB formation was slow. For example, the reaction between $LiBH_4$ and Mg_2FeH_6 in the $x = 0.5$ composite required more than 5 h to achieve a total hydrogen release of 3 mass %. The slow kinetics also caused the dehydrogenation process observed in the TG–MS and PCT measurements to exhibit different features. During the PCT measurements, the reaction between $LiBH_4$ and Mg_2FeH_6 can be separated from the dehydrogenation of MgH_2 for $x = 0.5$ and 0.75 because of the long reacting time. On the other hand, the high heating rate of 5 K·min^{-1} during the TG measurements in our previous report was not sufficient to incubate the reaction at its thermodynamically equilibrium temperature. According to theoretical data, it should be below 512 K (the equilibrium termperature at 0.1 MPa H_2) [23,25–27], but in our previous work, the dehydrogenation of the composite materials was observed beyond 630 K. At this temperature, MgH_2 was so unstable that the independent dehydrogenation of MgH_2 no longer occurred. The thermodynamic property of Mg_2FeH_6 is similar to that of MgH_2 [27]; thus, in the Mg_2FeH_6-rich compositions, independent dehydrogenation of Mg_2FeH_6 also no longer occurred and only one event appeared in the TG measurements for $x \geq 0.5$, with which all of the hydrogen-containing species dehydrogenated simultaneously. $LiBH_4$ is stable at the temperature of the simultaneous dehydrogenation. Therefore, for the $x < 0.5$ composite, the residue $LiBH_4$ reacted with Mg or dehydrogenated independently after the simultaneous dehydrogenation in which several dehydrogenation events were observed. The activation energy of the reaction between $LiBH_4$ and Mg_2FeH_6 should be different at the equilibrium reaction pressure and in the dynamic measurement. The detailed investigation will be carried out in a further study.

Ghaani et al. reported a composite reaction similar to that shown in Equation (2) in the $LiBH_4$-rich composition [13,19]. Our results demonstrate that the reaction between $LiBH_4$ and Mg_2FeH_6 was stoichiometric and did not degrade when excess $LiBH_4$ or Mg_2FeH_6 was present. Also, an optimal

composition ratio existed: $x = 0.5$, with which the independent dehydrogenation of the parent complex hydrides was avoided.

At the PCT experiment temperature of 643 K, the equilibrium pressure of the reaction between $LiBH_4$ and Mg_2FeH_6 is 38 times or 4 times higher than that of the dehydrogenation reaction of pure $LiBH_4$ or Mg_2FeH_6. This result indicates that both $LiBH_4$ and Mg_2FeH_6 were thermodynamically destabilized in the composite. In other composite materials, such as that between $LiBH_4$ and MgH_2, only $LiBH_4$ could be destabilized [3,20]. Another merit is that the H_2 capacity and the dehydrogenation process remained stable even under an Ar atmosphere. For example, for $x = 0.5$ composite, all the H_2 (6 mass %) was released in the temperature range 580 K to 630 K in the TG–MS experiments. However, an initial backpressure of at least 0.5 MPa H_2 is needed for the incubation of the composite reaction between $LiBH_4$ and MgH_2 [31,32]. Also, the dehydrogenation process of the composite material of $LiBH_4$ and Mg_2NiH_4 separated into more than three reactions and lasted from room temperature to beyond 673 K [6].

Full rehydrogenation of $x = 0.5$ composite requires much lower temperatures and pressures than those required in the partial rehydrogenation of $LiBH_4$ (pressures as high as 35 MPa H_2 and temperatures as high as 823 K [33]). Because previous studies on $LiBH_4$-rich compositions did not achieve full rehydrogenation, we consider that the optimal ratio contributed to the good reversible hydrogenation performance of the composite material [17,19,34].

4. Materials and Methods

4.1. Synthesis of $(1 - x)LiBH_4 + xMg_2FeH_6$

The synthesis of $(1 - x)LiBH_4 + xMg_2FeH_6$ ($x = 0.25$, 0.5, and 0.75) occurred via ball milling of commercially available $LiBH_4$ (purity $\geq$ 90%, Sigma-Aldrich, St. Louis, MO, USA) with laboratory-synthesized Mg_2FeH_6 (purity $\geq$ 90%) in an Ar atmosphere. The detailed synthesis method is described in the previous paper [12].

4.2. Pressure–Composition–Isothermal (PCT) Measurements

PCT measurements were conducted using a Sievert-type apparatus (Suzuki Shokan Co. Ltd., Tokyo, Japan, High-Pressure System Co., Saitama, Japan). The composite materials were heated to the designated temperature under a high H_2 pressure (>10 MPa) to prevent decomposition before the measurements. During the dehydrogenation measurements, H_2 was released in increments smaller than 0.01 MPa. The pressure change was kept stable between 15 min and 5 h to allow equilibration of the reaction at each step. Hydrogen weight loss was calculated using the function related to the pressure; volume of the apparatus, container, and material; and the temperatures at each part of the apparatus. The investigated temperature range was from 623 K to 673 K. The investigation of the rehydrogenation and reversible hydrogenation property of the optimized composition was performed in two steps. First, the dehydrogenation reaction was measured via PCT measurements using the same process described previously. Second, 20 MPa H_2 was added to the container, which was subsequently maintained for 20–24 h at the same temperature. This two-step process was repeated four times.

4.3. Phase Identification

Phase identification was performed using powder XRD (PANalytical X'Pert-Pro, Almelo, The Netherlands, Cu Kα radiation, λ = 1.5405 Å) at room temperature. The microstructure and element distributions of the synthesized samples and the dehydrogenated products were recorded via SEM (JSM-6009, JEOL Ltd., Tokyo, Japan) using an instrument equipped for EDS (EX-54175JMH, JEOL Ltd., Tokyo, Japan). During the synthesis and measurement processes, the samples were always handled under Ar or vacuum to avoid contamination by air or water.

5. Conclusions

The isothermal dehydrogenation processes of $(1 - x)LiBH_4 + xMg_2FeH_6$ (x = 0.25, 0.5, and 0.75) composite materials were studied using PCT measurements. The PCT results suggest that a stoichiometric reaction between $LiBH_4$ and Mg_2FeH_6 occurred at all of the investigated composition ratios, i.e., $LiBH_4 + Mg_2FeH_6 \rightarrow LiH + 2MgH_2 + (Fe, FeB) + 5/2H_2$. Both $LiBH_4$ and Mg_2FeH_6 were thermodynamically destabilized by this reaction. x = 0.5 is the optimal ratio for the composite material, which is also the reacting ratio of the two complex hydrides in the stoichiometric reaction. With the optimal ratio, the independent dehydrogenation of the excessive $LiBH_4$ or Mg_2FeH_6 was avoided. During the dynamic TG–MS experiments, only one dehydrogenation event was observed for the x = 0.5 and 0.75 composites. The difference between the PCT and TG–MS results is explained by the slow kinetics of the reaction between $LiBH_4$ and Mg_2FeH_6. Beside the dehydrogenation property, the optimal ratio also contributed to the enhanced reversible hydrogenation properties of the composite materials. The x = 0.5 composites can be de/rehydrogenated completely at 673 K and 20 MPa H_2 for at least four cycles without the loss of H_2 capacity.

Acknowledgments: This research has been financed by the Grant-in-Aid for Young Scientists (B) (17K14830), the Grant-in-Aid for Research Fellow of Japan Society for the Promotion of Science (15J10604), the JSPS KAKENHI Grant (25220911), and the German Federal Government under the European ERA-NET CONCERT Japan scheme via the iTHEUS project (grant CONCERT-EN-015). The authors would like to acknowledge Ms. N. Warifune for providing technical support.

Author Contributions: Guanqiao Li, Motoaki Matsuo, and Shin-ichi Orimo conceived and designed the experiments; Guanqiao Li and Anna-Lisa Chaudhary performed the experiments; Toyoto Sato and Shigeyuki Takagi helped analyze the data; Anna-Lisa Chaudhary and Martin Dornheim gave advice concerning the analysis of the data; and Guanqiao Li wrote the paper.

Conflicts of Interest: The authors declare no conflict of interest.

References

1. Paskevicius, M.; Jepsen, L.H.; Schouwink, P.; Cerny, R.; Ravnsbaek, D.B.; Filinchuk, Y.; Dornheim, M.; Besenbacher, F.; Jensen, T.R. Metal Borohydrides and Derivatives—Synthesis, Structure and Properties. *Chem. Soc. Rev.* **2017**, *46*, 1565–1634. [CrossRef] [PubMed]
2. Callini, E.; Atakli, Z.O.K.; Hauback, B.C.; Orimo, S.; Jensen, C.; Dornheim, M.; Grant, D.; Cho, Y.W.; Chen, P.; Hjorvarsson, B.; et al. Complex and Liquid Hydrides for Energy Storage. *Appl. Phys. A* **2016**, *122*, 353. [CrossRef]
3. Orimo, S.; Nakamori, Y.; Eliseo, J.R.; Zuttel, A.; Jensen, C.M. Complex Hydrides for Hydrogen Storage. *Chem. Rev.* **2007**, *107*, 4111–4132. [CrossRef] [PubMed]
4. Li, H.W.; Yan, Y.G.; Orimo, S.; Züttel, A.; Jensen, C.M. Recent Progress in Metal Borohydrides for Hydrogen Storage. *Energies* **2011**, *4*, 185–214. [CrossRef]
5. Bösenberg, U.; Doppiu, S.; Mosegaard, L.; Barkhordarian, G.; Eigen, N.; Borgschulte, A.; Jensen, T.R.; Cerenius, Y.; Gutfleisch, O.; Klassen, T.; et al. Hydrogen Sorption Properties of MgH_2–$LiBH_4$ Composites. *Acta Mater.* **2007**, *55*, 3951–3958. [CrossRef]
6. Vajo, J.J.; Li, W.; Liu, P. Thermodynamic and Kinetic Destabilization in $LiBH_4$–Mg_2NiH_4: Promise for Borohydride-Based Hydrogen Storage. *Chem. Commun.* **2010**, *46*, 6687–6689. [CrossRef] [PubMed]
7. Javadian, P.; Zlotea, C.; Ghimbeu, C.M.; Latroche, M.; Jensen, T.R. Hydrogen Storage Properties of Nanoconfined $LiBH_4$–Mg_2NiH_4 Reactive Hydride Composites. *J. Phys. Chem. C* **2015**, *119*, 5819–5826. [CrossRef]
8. Yan, Y.G.; Li, H.W.; Maekawa, H.; Miwa, K.; Towata, S.; Orimo, S. Formation of Intermediate Compound $Li_2B_{12}H_{12}$ during The Dehydrogenation Process of The $LiBH_4$–MgH_2 System. *J. Phys. Chem. C* **2011**, *115*, 19419–19423. [CrossRef]
9. Bergemann, N.; Pistidda, C.; Milanese, C.; Emmler, T.; Karimi, F.; Chaudhary, A.L.; Chierotti, M.R.; Klassen, T.; Dornheim, M. $Ca(BH_4)_2$–Mg_2NiH_4: On The Pathway to A $Ca(BH_4)_2$ System with A Reversible Hydrogen Cycle. *Chem. Commun.* **2016**, *52*, 4836–4839. [CrossRef] [PubMed]

10. Bosenberg, U.; Kim, J.W.; Gosslar, D.; Eigen, N.; Jensen, T.R.; von Colbe, J.M.B.; Zhou, Y.; Dahms, M.; Kim, D.H.; Gunther, R.; et al. Role of Additives in $LiBH_4$–MgH_2 Reactive Hydride Composites for Sorption Kinetics. *Acta Mater.* **2010**, *58*, 3381–3389. [CrossRef]
11. Yang, J.; Sudik, A.; Wolverton, C. Destabilizing $LiBH_4$ with A Metal (M = Mg, Al, Ti, V, Cr, or Sc) or Metal Hydride (MH_2, MgH_2, TiH_2, or CaH_2). *J. Phys. Chem. C* **2007**, *111*, 19134–19140. [CrossRef]
12. Li, G.; Matsuo, M.; Deledda, S.; Sato, R.; Hauback, B.C.; Orimo, S. Dehydriding Property of $LiBH_4$ Combined with Mg_2FeH_6. *Mater. Trans.* **2013**, *54*, 1532–1534. [CrossRef]
13. Li, G.; Matsuo, M.; Aoki, K.; Ikeshoji, T.; Orimo, S. Dehydriding Process and Hydrogen-Deuterium Exchange of $LiBH_4$–Mg_2FeD_6 Composites. *Energies* **2015**, *8*, 5459–5466. [CrossRef]
14. Chaudhary, A.-L.; Li, G.; Matsuo, M.; Orimo, S.; Deledda, S.; Sørby, M.H.; Hauback, B.C.; Pistidda, C.; Klassen, T.; Dornheim, M. Simultaneous Desorption Behavior of M Borohydrides and Mg_2FeH_6 Reactive Hydride Composites (M = Mg, then Li, Na, K, Ca). *Appl. Phys. Lett.* **2015**, *107*, 073905. [CrossRef]
15. Li, G.; Matsuo, M.; Deledda, S.; Hauback, B.C.; Orimo, S. Dehydriding Property of $NaBH_4$ Combined with Mg_2FeH_6. *Mater. Trans.* **2014**, *55*, 1141–1143. [CrossRef]
16. Pinkerton, F.E.; Meyer, M.S.; Meisner, G.P.; Balogh, M.P.; Vajo, J.J. Phase Boundaries and Reversibility of $LiBH_4$–MgH_2 Hydrogen Storage Material. *J. Phys. Chem. C* **2007**, *111*, 12881–12885. [CrossRef]
17. Deng, S.S.; Xiao, X.Z.; Han, L.Y.; Li, Y.; Li, S.Q.; Ge, H.W.; Wang, Q.D.; Chen, L.X. Hydrogen Storage Performance of $5LiBH_4$ + Mg_2FeH_6 Composite System. *Int. J. Hydrog. Energy* **2012**, *37*, 6733–6740. [CrossRef]
18. Langmi, H.W.; McGrady, G.S.; Newhouse, R.; Rönnebro, E. Mg_2FeH_6–$LiBH_4$ and Mg_2FeH_6–$LiNH_2$ Composite Materials for Hydrogen Storage. *Int. J. Hydrog. Energy* **2012**, *37*, 6694–6699. [CrossRef]
19. Ghaani, M.R.; Catti, M.; Nale, A. Thermodynamics of Dehydrogenation of the $2LiBH_4$–Mg_2FeH_6 Composite. *J. Phys. Chem. C* **2012**, *116*, 26694–26699. [CrossRef]
20. Bogdanovic, B.; Bohmhammel, K.; Christ, B.; Reiser, A.; Schlichte, K.; Vehlen, R.; Wolf, U. Thermodynamic Investigation of the Magnesium–Hydrogen System. *J. Alloys Compd.* **1999**, *282*, 84–92. [CrossRef]
21. Bohmhammel, K.; Wolf, U.; Wolf, G.; Konigsberger, E. Thermodynamic Optimization of the System Magnesium–Hydrogen. *Thermochim. Acta* **1999**, *337*, 195–199. [CrossRef]
22. Zhang, X.; Yang, R.; Qu, J.; Zhao, W.; Xie, L.; Tian, W.; Li, X. The Synthesis and Hydrogen Storage Properties of Pure Nanostructured Mg_2FeH_6. *Nanotechnology* **2010**, *21*, 095706. [CrossRef] [PubMed]
23. Puszkiel, J.A.; Larochette, P.A.; Gennari, F.C. Thermodynamic and Kinetic Studies of Mg–Fe–H after Mechanical Milling Followed by Sintering. *J. Alloys Compd.* **2008**, *463*, 134–142. [CrossRef]
24. Wang, Y.; Cheng, F.Y.; Li, C.S.; Tao, Z.L.; Chen, J. Preparation and Characterization of Nanocrystalline Mg_2FeH_6. *J. Alloys Compd.* **2010**, *508*, 554–558. [CrossRef]
25. Siegel, D.J.; Wolverton, C.; Ozoliņš, V. Thermodynamic Guidelines for the Prediction of Hydrogen Storage Reactions and Their Application to Destabilized Hydride Mixtures. *Phys. Rev. B* **2007**, *76*. [CrossRef]
26. Price, T.E.C.; Grant, D.M.; Telepeni, I.; Yu, X.B.; Walker, G.S. The Decomposition Pathways for $LiBD_4$–MgD_2 Multicomponent Systems Investigated by In Situ Neutron Diffraction. *J. Alloys Compd.* **2009**, *472*, 559–564. [CrossRef]
27. Miwa, K.; Takagi, S.; Matsuo, M.; Orimo, S. Thermodynamical Stability of Complex Transition Metal Hydrides M_2FeH_6. *J. Phys. Chem. C* **2013**, *117*, 8014–8019. [CrossRef]
28. Bogdanovic, B.; Reiser, A.; Schlichte, K.; Spliethoff, B.; Tesche, B. Thermodynamics and Dynamics of the Mg−Fe−H System and Its Potential for Thermochemical Thermal Energy Storage. *J. Alloys Compd.* **2002**, *345*, 77–89. [CrossRef]
29. Zavorotynska, O.; Corno, M.; Damin, A.; Spoto, G.; Ugliengo, P.; Baricco, M. Vibrational Properties of MBH_4 and MBF_4 Crystals (M = Li, Na, K): A Combined DFT, Infrared, and Raman Study. *J. Phys. Chem. C* **2011**, *115*, 18890–18900. [CrossRef]
30. Parker, S.F.; Williams, K.P.J.; Bortz, M.; Yvon, K. Inelastic Neutron Scattering, Infrared, and Raman Spectroscopic Studies of Mg_2FeH_6 and Mg_2FeD_6. *Inorg. Chem.* **1997**, *36*, 5218–5221. [CrossRef]
31. Kim, K.B.; Shim, J.H.; Park, S.H.; Choi, I.S.; Oh, K.H.; Cho, Y.W. Dehydrogenation Reaction Pathway of the $LiBH_4$−MgH_2 Composite under Various Pressure Conditions. *J. Phys. Chem. C* **2015**, *119*, 9714–9720. [CrossRef]
32. Bosenberg, U.; Ravnsbaek, D.B.; Hagemann, H.; D'Anna, V.; Minella, C.B.; Pistidda, C.; van Beek, W.; Jensen, T.R.; Bormann, R.; Dornheim, M. Pressure and Temperature Influence on the Desorption Pathway of the $LiBH_4$−MgH_2 Composite System. *J. Phys. Chem. C* **2010**, *114*, 15212–15217. [CrossRef]

33. Orimo, S.; Nakamori, Y.; Kitahara, G.; Miwa, K.; Ohba, N.; Towata, S.; Zuttel, A. Dehydriding and Rehydriding Reactions of $LiBH_4$. *J. Alloys Compd.* **2005**, *404*, 427–430. [CrossRef]
34. Gosselin, C.; Deledda, S.; Hauback, B.C.; Huot, J. Effect of Synthesis Route on the Hydrogen Storage Properties of $2MgH_2$–Fe Compound Doped with $LiBH_4$. *J. Alloys Compd.* **2015**, *645*, S304–S307. [CrossRef]